Surface Trapped X Rays: Whispering-Gallery Modes at $\lambda = 0.7$ Å

Chien Liu[1] and Jene A. Golovchenko[1,2,3]
[1]*Division of Engineering and Applied Sciences, Harvard University, Cambridge, Massachusetts 02138*
[2]*Department of Physics, Harvard University, Cambridge, Massachusetts 02138*
[3]*Rowland Institute for Science, Cambridge, Massachusetts 02142*
(Received 16 May 1997)

X-ray bound states trapped on a curved surface are realized by coupling subangstrom photons at grazing angles into a bent silicon wafer with adjustable radius. At small radii of curvature the usual ray approximation breaks down and new phenomena associated with wave optical behavior of x-ray surface eigenmodes are revealed. For such samples, tunneling is shown to extinguish all but the ground state surface eigenmode, whose presence may be detected after extremely long distances of propagation along the surface. [S0031-9007(97)03712-5]

PACS numbers: 07.85.Fv, 41.50.+h

The impact x-ray physics has had upon almost all areas of modern science can hardly be overstated. The continuing investment in, and development of, new sources of intense and even coherent x-ray radiation as well as the refinement and extension of methods to probe matter with these sources attests to the continuing importance of this field. A remarkably large fraction of the phenomena associated with x-ray propagation in matter can be accounted for by Maxwell mean field equations, within which the influence of atomic matter is made manifest by a frequency and space dependent complex dielectric function.

Despite the fact that relatively small spatial modulations of the refractive index are obtained at very short (<1 Å) wavelengths [1], under special circumstances it is possible to dramatically transform and manipulate x-ray fields when the interaction region is large enough. This occurs, for example, when x rays are totally reflected from flat surfaces at grazing incidence as described by the Fresnel laws of refraction and reflection for plane waves [2] and when dynamical diffraction effects are obtained as a result of x rays propagating large distances in very perfect crystal structures [3]. Modern methods of materials science have recently been applied to prepare artificial multilayer crystals [4] as well as multiple total reflection waveguides [5] that manipulate and transform x-ray beams in related ways.

In the following we demonstrate that wave optical guiding effects can be obtained in a very simple curved mirror geometry for very short wavelength x rays. Eigenmodes of the mean field equation are observed after centimeter propagation distances for states that are confined within a thousand angstroms of the waveguide surface. These results suggest the possibility of a wide variety of new two dimensional wave optical x-ray phenomena on curved surfaces.

The application of curved reflecting structures in x-ray physics has recently been reviewed [6] with particular emphasis on the ray optics of such devices. At small radii of curvature this model breaks down and a wave mechanical view is required. We show that propagation is then connected with a phenomenon analogous to the whispering gallery modes, first discussed in acoustics [7]. In the soft x-ray regime there has been much theoretical and some experimental work in exploring the possibility of using the whispering-gallery effect to achieve focusing, deflection, and circular polarization of x rays, and even the construction of resonant cavities for laser operation [8]. In the following we describe both our theoretical and experimental investigation of the propagation of hard x rays ($\lambda < 1$ Å) in the whispering gallery modes. In particular, we will show how the ray-optical picture breaks down at sufficiently small radii of curvature and how new phenomena like tunneling and surface diffraction effects can become important. In addition to potential applications as x-ray optical elements and surface probes, the curved surface geometry offers a unique model for studying wave propagation in a warped space.

Figure 1 shows a schematic side view of a whispering-gallery waveguide, which is made from a thin silicon wafer. The waveguide is mounted on a holder with a

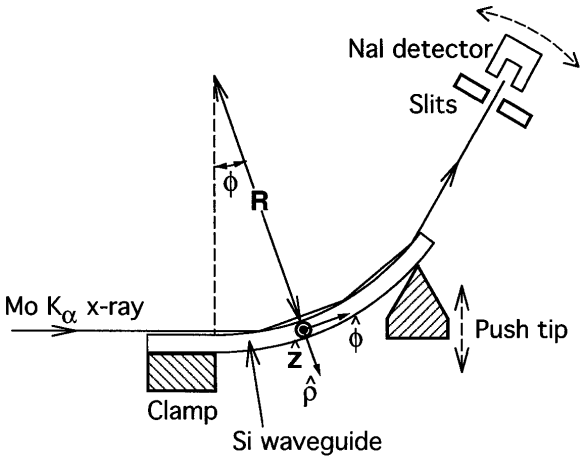

FIG. 1. Schematic side view of a whispering-gallery waveguide made from a thin silicon wafer. The radius of curvature of the waveguide is controlled by the push tip. A grazing incident x ray is depicted as a ray propagating along the curved surface through three successive reflections.

 0031-9007/97/79(5)/788(4)$10.00

fixed clamp and a movable push tip that produces an adjustable radius of curvature in the silicon surface. In a ray-optical picture the parallel incident x-ray beam is divided transversely into an infinite number of rays. Each ray goes through successive specular reflections on the curved waveguide surface, as illustrated in the figure. The reflectivity of each bounce is given by the Fresnel formulas [2]. Consider Mo K_α radiation ($\lambda = 0.7$ Å) on a Si waveguide with 10 cm radius and 1 cm arc length as an example. Below the critical angle, $\theta_c = 0.1°$ [1], the reflectivity is close to unity, and the loss of x-ray intensity in this picture comes from absorption. For the ray entering the waveguide at half of the critical angle, $\theta_c/2 = 0.05°$, the reflectivity given by the Fresnel formula is $R = 99.4\%$. After 55 successive reflections on the surface (corresponding to the 1 cm arc length) the probability of survival is $R^{55} = 71\%$. Integration of all rays entering below the critical angle θ_c shows that about 60% of the x-ray photons will survive after 1 cm travel on the waveguide surface. Because θ_c is very small, the ray which enters at θ_c is only 1600 Å above the waveguide surface. (In comparison a "narrow" x-ray beam prepared using commonly available slits has a width on the order of 10 μm. Therefore the transmittance in a typical experiment is the order of $60\% \times 1600$ Å$/10$ μm $= 1\%$.)

To demonstrate conditions under which the above simple description is satisfactory we measured the transmittance as a function of the radius of curvature (controlled by the push tip position) for waveguides made from thin Si(111) wafers, which were Syton polished to a haze-free mirror finish by Virginia Semiconductor, Inc. The waveguides were formed in triangular shapes to achieve approximately constant radius of curvature across the surface [9]. A monochromatic Mo K_α x-ray beam from a rotating anode x-ray machine was coupled into the waveguide at a grazing angle (see Fig. 1). The incident beam ($\sim 10^5$ photons/sec) was 20 μm wide in the out-of-plane ($\hat{\rho}$) direction and collimated to 0.0009° by a Bragg reflection from a symmetrically cut Si(111) crystal. It was 2 mm wide with 0.3° divergence in the in-plane ($\hat{z}$) direction. The incident and exiting x-ray intensities and the deflection angle at each push tip position were measured by a collimated NaI detector. Figure 2 shows the exiting x-ray intensity normalized by the total incident intensity (the transmittance) versus the push tip position for an 18 mm long 100 μm thick Si waveguide. The largest deflection angle of the exiting x-ray beam for this waveguide was 13°. The statistical uncertainty in the count rate and the uncertainty in measuring the x-ray beam width (and therefore the intensity per area) determine the error bars in the transmittance shown in the figure. The solid curve in the figure shows the prediction from ray tracing calculations based on the Fresnel formulas. For the purpose of ray tracing, the detailed shape of the Si waveguide at each push tip position was obtained by scanning a He-Ne laser beam across the Si surface and measuring the reflection angles. The radius of curvature was found to range from 80 to 10 cm for various push tip positions. The ray-optical approximation works well in this regime.

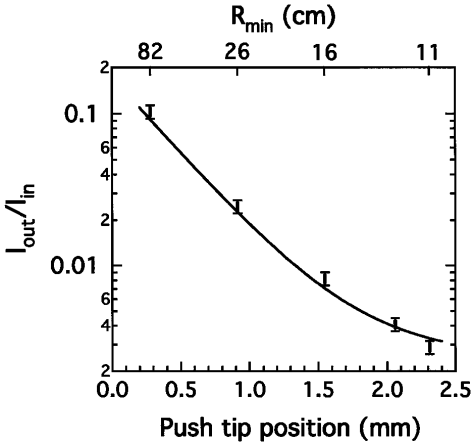

FIG. 2. Transmittance versus the push tip position and minimum radius of curvature ($R_{\min}$) for Mo K_α radiation on a bent 18 mm long Si mirror. Solid curve is the prediction from ray tracing calculations.

This, however, is not the case for the data in Fig. 3. It shows the transmittance versus the push tip position for a 5 mm long and 50 μm thick Si waveguide, which could be bent to a smaller radius of curvature. The largest deflection angle of the exiting x-ray beam for this waveguide was 8°. The shape of this waveguide was determined by imaging it, edge on, under an optical microscope. The radii of curvature ranged from 15 to 1 cm for various push tip positions. The transmittance data for this waveguide shows a steep drop with decreasing radius of curvature (higher push tip position) and it deviates significantly from the ray-optical prediction (the dotted curve). To explain such a steep change of the transmittance, the propagation of the x rays on a waveguide has to be reexamined using the wave-optical theory.

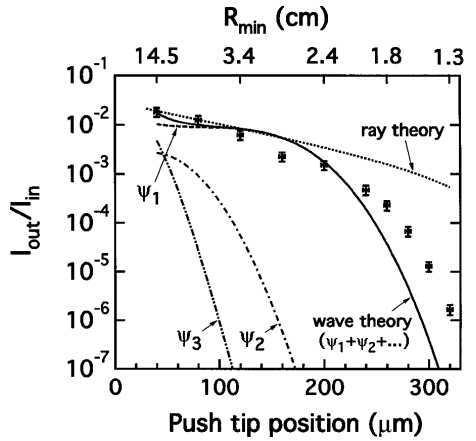

FIG. 3. Transmittance for a 5 mm long Si mirror. Dotted and solid curves are predictions from a ray tracing calculation and a simple wave-optical model, respectively. Dashed and dash-dotted curves ψ_1, ψ_2, and ψ_3 are calculated contributions from the three lowest bound states in the wave-optical model.

We start by solving the Maxwell equations in the cylindrical coordinates (ρ, φ, z) defined by a cylindrical mirror surface with radius R (see Fig. 1). The dielectric function ε is 1 for $\rho < R$ and $1 - 3.16 \times 10^{-6} + 1.71 \times 10^{-8} i$ for $\rho > R$ [1]. For x rays in the vicinity of the curved mirror surface, the wave equation can be separated and cast in a form similar to the well known Schrödinger equation from quantum mechanics. Consider as an example the case where the x ray propagates in the azimuthal $(\hat{\phi})$ direction and the polarization of the electric field is parallel to the axial $(\hat{z})$ direction (along the cylinder axis). With the substitution

$$E_z(\rho, \phi, z, t) \equiv \psi(y) \frac{e^{i\nu\phi - i\omega t}}{y + R}, \quad y \equiv \rho - R, \quad (1)$$

the wave equation for the E field near the surface becomes

$$-\psi'' + \left(k_0^2[1 - \varepsilon(y)] - \frac{2\nu^2 y}{R^3}\right)\psi = \left(k_0^2 - \frac{\nu^2}{R^2}\right)\psi, \quad (2)$$

where $k_0 \equiv \omega/c = 2\pi/\lambda$ is the vacuum wave vector, and λ is the vacuum wave length of the x ray. This equation is valid only in the region $|y| \ll R$, which will be shown to be a good approximation for the surface x-ray waves. Equation (2) has the same form as a *time-independent* Schrödinger equation,

$$-\psi'' + \frac{2m}{\hbar^2} V(y)\psi = \frac{2m}{\hbar^2} E\psi. \quad (3)$$

For Mo K_α x rays on a Si waveguide with 10 cm radius, the effective potential $V(y)$ and some of the corresponding ψ's for the x rays near the mirror surface are shown in Fig. 4. Note that the range of y is ± 2000 Å, much less than $R = 10$ cm. The potential is characterized by an effective centrifugal barrier punctuated by a positive step at the mirror surface. Clearly long-lived quasibound states should exist in the effective potential well (region I) just outside the mirror surface. These "bound states" correspond to the whispering-gallery x-ray waveguide eigenmodes. As shown in Fig. 4 the x-ray intensity in each eigenmode is concentrated in a region less than 1500 Å wide just outside the mirror surface. The classically forbidden region II, below the surface, is penetrated less than 100 Å by a tunneling evanescent tail. The fact that these modes spend a significant part of their time outside the surface indicates a reduced absorption effect. For example, the $1/e$ attenuation distance for the ground state is 2.8 cm, compared to 0.066 cm for x rays propagating in the Si bulk. The fact that these x-ray modes interact only with the surface region, and over a very long distance, suggests they will find application as a sensitive surface probe.

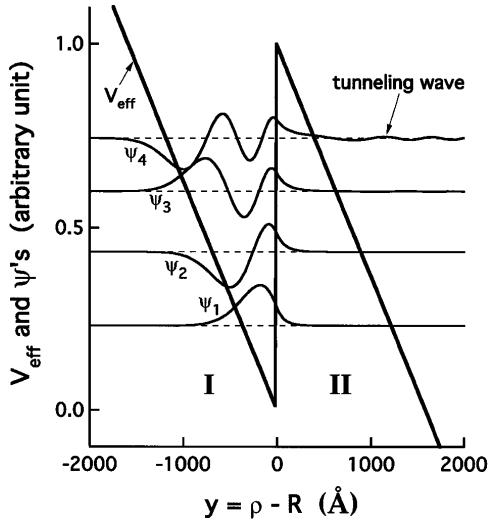

FIG. 4. Effective potential and the corresponding wave solutions for x rays near a 10 cm radius mirror surface.

Each wave function in Fig. 4 is positioned vertically according to its effective total energy in the Schrödinger equation analogy. The outgoing tunneling wave of the highest wave function ψ_4 in the figure can be seen for $y > 0$, while the first three wave functions appear to be well confined near the mirror surface. In general, the behavior of the x-ray waveguide mode is controlled by the effective potential near the mirror surface. The height of the effective potential step at $y = 0$ is proportional to the difference in dielectric constant ε across the mirror surface. The widths of the potential well (region I) and the potential barrier (region II) are both proportional to the radius of curvature R. For a waveguide with a smaller radius R the narrower well accommodates fewer bound states, and the thinner barrier allows more tunneling. In this limit the ray-optical theory breaks down and the wave-optical description becomes necessary. For $R \leq 3$ cm, only one bound state is allowed in the potential well, and the loss of x-ray intensity is dominated by the tunneling effect.

The solid curve in Fig. 3 shows the transmittance predicted by a simple wave-optical calculation based on the adiabatic approximation, valid when the radius of curvature varies slowly across the surface. The incident x-ray beam is assumed to be a plane wave that couples into the waveguide eigenmodes. Each mode is assumed to continuously transform to occupy an eigenmode associated with the local radius of curvature at each point on the surface. The intensities of the eigenmodes after propagating through the waveguide (the dashed and dash-dotted curves marked as ψ_1, ψ_2, and ψ_3), accounting for tunneling and absorption, are added to give an estimate of the total exiting x-ray intensity (the solid curve). The steep drop in transmittance toward smaller radius of curvature in Fig. 3 agrees qualitatively with the data. Clearly the contributions from all excited states $(\psi_2, \psi_3, \ldots)$ effectively vanish for push tip position larger than 120 μm and single mode (ground state ψ_1) conditions have been achieved for most of the data in Fig. 3.

The discrepancy is attributed to several idealizations used in the model for the wave-optical calculation. The air-mirror interface was assumed to be infinitely sharp, ignoring the effect of possible contaminates and roughness on the mirror surface. The incident beam divergence in the

$\hat{z}$ direction was also neglected in the calculation. Most importantly, the determination of the waveguide shape is crucial, since the tunneling effect is exponentially sensitive to the barrier width ($\propto R$). The bending of the waveguide in the $\hat{\phi}$ direction also introduces a curvature in the $\hat{z}$ direction known as anticlastic bending [10]. The metrical structure of this complex surface (effectively a 2D non-Euclidean space) must surely affect the two dimensional propagation of the bound surface x-ray states, but a careful experimental and theoretical study requires further research.

An alternative way to deal with the propagation of whispering gallery x-ray waves has been developed by Braud and Hagelstein [11]. (A similar approach has also been used for the description of electron channeling effects [12].) Here the fast ϕ dependence of the wave function is factored out, leaving a wave equation that closely resembles the *time-dependent* Schrödinger equation. We have used Crank-Nicholson methods [13] to integrate this equation for small radii of curvature where tunneling losses are the greatest. The calculated attenuation factor of a ground state eigenmode propagating across the waveguide surface at the push tip position of 320 μm agrees with the value obtained from the adiabatic approximation to within 1%. For large radii of curvature this method becomes impractical because the required spatial integration range grows beyond the memory capacity of an ordinary personal computer.

To conclude we suggest that the surface-sensitive whispering-gallery eigenmodes discussed in this paper can provide new possibilities for the study of clean surfaces, interfaces, and adsorbed molecules with hard x rays. The in-surface diffraction of whispering gallery modes by periodic arrays of atoms or molecules on the surface should yield particularly strong effects. From a more general perspective there appears to be significant prospects for developing the optics of x rays, bound to a two dimensional manifold, within which surface curvature and composition control the evolution of photon states.

We thank Dr. M. Burns and Dr. L. Hau at the Rowland Institute for Science, Dr. M. R. Howells at Lawrence Berkeley Laboratory, and Professor E. Kaxiras at Harvard University for their useful discussions and assistance. This work is supported by the Joint Services Electronics Program (JSEP N00014-89-J-1023) and the Materials Research Laboratory at Harvard (NSF-DMR-8920490).

[1] *International Tables for X-ray Crystallography,* edited by J. A. Ibers and W. C. Hamilton (Kynoch Press, Birmingham, 1974), Vol. IV.

[2] J. D. Jackson, *Classical Electrodynamics* (Wiley, New York, 1975), 2nd ed., pp. 278–282.

[3] B. W. Batterman and H. Cole, Rev. Mod. Phys. **36**, 681 (1964).

[4] *Multilayer Optics for Advanced X-Ray Applications*, edited by N. M. Ceglio, SPIE Proc. Vol. 1547 (SPIE, Bellingham, WA, 1992).

[5] M. A. Kumakhov and F. F. Komarov, Phys. Rep. **191**, 289 (1990); J. Wang, M. J. Bedzyk, and M. Caffrey, Science **258**, 775 (1992); Y. P. Feng, S. K. Sinha, H. W. Deckman, J. B. Hastings, and D. P. Siddons, Phys. Rev. Lett. **71**, 537 (1993).

[6] D. H. Bilderback and D. J. Thiel, Rev. Sci. Instrum. **66**, 2059 (1995).

[7] Lord Rayleigh, *The Theory of Sound*, first published 1877; American edition: Dover, New York, 1945.

[8] See, for example, I. N. Bukreva, I. V. Kozhevnikov, and A. V. Vinogradov, SPIE **2453**, 80 (1995); N. V. Smith and M. R. Howells, Nucl. Instrum. Methods Phys. Res., Sect. A **347**, 115 (1994); J. P. Braud and P. L. Hagelstein, IEEE J. Quantum Electron. **27**, 1069 (1991), and references therein.

[9] M. Lemonnier, R. Fourme, F. Rousseaux, and R. Kahn, Nucl. Instrum. Methods **152**, 173 (1978).

[10] S. P. Timoshenko and J. N. Goodier, *Theory of Elasticity* (McGraw-Hill, New York, 1969), 3rd ed., pp. 284–288.

[11] J. P. Braud and P. L. Hagelstein, IEEE J. Quantum Electron. **28**, 254 (1992).

[12] See, for example, P. Lervig, J. Lindhard, and V. Nielsen, Nucl. Phys. **A96**, 481 (1967).

[13] S. E. Koonin, *Computational Physics* (Addison-Wesley, Reading, 1990).